

## Formation of Arrays of Straight Copper Wires on Solid Substrate by Electrodeposition

Sheng ZHONG, Mu WANG\*, Xiao-Bo YIN, Jian-Ming ZHU,  
Ru-Wen PENG, Yuan WANG and Nai-Ben MING

*National Laboratory of Solid State Microstructures and Department of Physics,  
Nanjing University, Nanjing 210093, China*

(Received September 18, 2000)

Straight copper wire arrays are electrochemically deposited on a silicon substrate without utilizing additives or templates. To suppress the influence of the factors which arouse the ramification of the copper electrodeposit, an ultrathin electrochemical deposition system and an initially homogeneous electric field are used. The width of the copper wires may vary from about 200 nm to about 1.5  $\mu\text{m}$  depending on the control parameters. The microstructure of the copper wires and their electric resistance after vacuum-annealing at 200°C are studied. We suggest that this self-organized copper electrodeposition is helpful in gaining an understanding of the formation of dense-branching morphology. It also implies the potential application in microelectronics.

KEYWORDS: copper electrodeposition, pattern formation, electrochemical methodes

Recently, electrochemical metallization of copper has been developed for on-chip interconnection in microelectronics.<sup>1,2)</sup> Compared to the Ti/Al(Cu) wiring, the copper wiring has the advantages of significantly lower resistance, higher allowed current density and increased scalability.<sup>3)</sup> In the microelectronics industry, the metallic interconnection is conventionally achieved by photolithography. To achieve a robust copper film on a solid substrate, special treatments have to be made on the solid surface. For example, as reported by Fleury and Barkey,<sup>4,5)</sup> an ultrathin, pre-coated metallic layer (non-percolated) helps the two-dimensional electrodeposition. Alternatively, organic additives are introduced<sup>6-8)</sup> and their effects on the interfacial growth are investigated. To find new ways to form contacts in three dimensions and to achieve enhanced data-processing density, researchers have been attempting to establish conducting channels between the electrodes either by patterned and direction-controlled electrodeposition<sup>9,10)</sup> or by electropolymerization.<sup>11,12)</sup> However in previous experiments the metal deposit was usually irregularly branched or fractal-like,<sup>4,10,13)</sup> which would affect the high-frequency electric properties of the metal connections. On the other hand, from the point of view of fundamental research, the branching mechanism in far-from-equilibrium growth remains a challenging problem in pattern formation.<sup>14-16)</sup> Conventionally, the branching of a growing tip has been associated with external disturbances.<sup>17-19)</sup> It is intriguing to consider whether the ramified feature remains in the electrodeposition when the external agitations are suppressed, and whether regular patterns can be directly electrodeposited on a solid substrate. Here we report a novel experiment which

demonstrates that copper wire arrays could be generated robustly on a silicon substrate directly by electrodeposition. No additives or templates were introduced in this process. The width of the copper wire could vary from 200 nm to about 1.5  $\mu\text{m}$  depending on the control parameters. The microstructures of the wires and the dynamic behavior of their resistance under annealing were also investigated.

The experimental setup for the copper electrodeposition is schematically shown in Fig. 1. The cell for the electrodeposition consisted of two parallel electrodes separated by 8.0 mm and fixed on the bottom glass plate. The anode was made of pure copper wire (99.9%, Goodfellow, U.K.) and the cathode was a graphite rod 0.5 mm in diameter. A piece of (100)-orientated silicon wafer (10 × 10 mm, p-Type, boron-doped, resistivity of

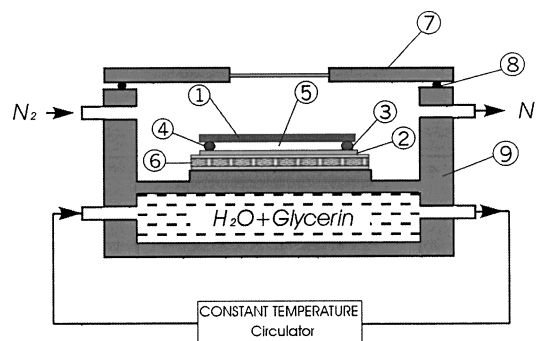


Fig. 1. Schematic diagram showing experimental setup. (1) silicon wafer (substrate); (2) bottom glass plate; (3) cathode; (4) anode; (5) electrolyte sandwiched between the silicon wafer and the bottom glass plate; (6) Peltier element; (7) top cover of thermostated chamber with a glass window; (8) rubber O-ring for sealing; (9) thermostated chamber to maintain the constant temperature for electrodeposition.

\*To whom correspondence should be addressed. E-mail: muwang@netra.nju.edu.cn

40  $\Omega \cdot \text{cm}$ ) was used as the top plate, on which the copper wire array was deposited, marked as **1** in Fig. 1. The electrolyte of  $\text{CuSO}_4$  (0.05 M,  $\text{pH}=4.5$ ) was sandwiched between the silicon wafer and the glass plate. The electrolyte solution was prepared by analytical reagent  $\text{CuSO}_4$  and de-ionized, ultrapure water (electric resistivity 17.8  $\text{M}\Omega \cdot \text{cm}$ ). No special treatments were made on the surfaces of either the bottom glass plate or the top silicon wafer except for the standard cleaning process. A Peltier element was placed beneath the electrodeposition cell to modify the temperature of the deposition cell. Both the deposition cell and the Peltier element were sealed in a thermostat chamber with dry nitrogen flow. The system was cooled to below the freezing point of the electrolyte. Meanwhile, solidification started from the bottom glass plate. Usually the temperature was set at  $-4^\circ\text{C}$  for the 0.05 M electrolyte. Great care had been taken to retain just one or only a few ice nuclei in the system and to avoid the formation of a cellular or dendritic ice-electrolyte interface during the solidification. Several melting-solidification cycles had to be repeated to fulfil these requirements. During the solidification of the electrolyte,  $\text{CuSO}_4$  was partially expelled from the solid (known as the partitioning effect<sup>20,21</sup>) in crystallization). Consequently a very thin layer of concentrated  $\text{CuSO}_4$  electrolyte was trapped between the ice of the electrolyte and the boundary of the cell (silicon substrate) when the cell was frozen. The copper electrodeposition was carried out in this ultrathin layer where the electrolyte concentration did not exceed the saturation concentration of  $-4^\circ\text{C}$ . At  $-4^\circ\text{C}$  the thickness of this layer was about 200 to 300 nm, which was estimated from the thickness of the copper deposit measured by atomic force microscopy. As illustrated in Fig. 1, two electrodes were in contact with this concentrated ultrathin electrolyte layer. This had been confirmed by measuring the electric resistance between the two electrodes when the solidification was completed. Meanwhile, the resistance of the system was several orders of magnitude smaller than that in the case when the electrodes were embedded in the bulk ice of the electrolyte of the same concentration.

After confirming that the potentiostatic and the galvanostatic experiments generated a similar deposit morphology, we adopted the potentiostatic design. A constant voltage was applied across the electrodes, which could be selected to be between 3.0 V and 10.0 V. The copper electrodeposit initiated from the cathode and grew on the silicon substrate. Figure 2(a) shows the morphology of the copper wires viewed by an atomic force microscope (AFM; Nanoscope IIIa, Digital Instruments, U.S.A.) after the growth. Unlike previously reported random branching morphology,<sup>4,10,13</sup> here the deposit consisted of many straight, smooth and fine filaments (wires), which were robustly grown on the silicon wafer. Tip-splitting did occur in some wires; however, the branching rate was significantly decreased compared with that of those grown in the conventional aqueous solution environment.<sup>4,10,13</sup> Figure 2(b) shows the detail morphology of the copper wire array on the silicon wafer, where the surface of the wires is smooth. Our experi-

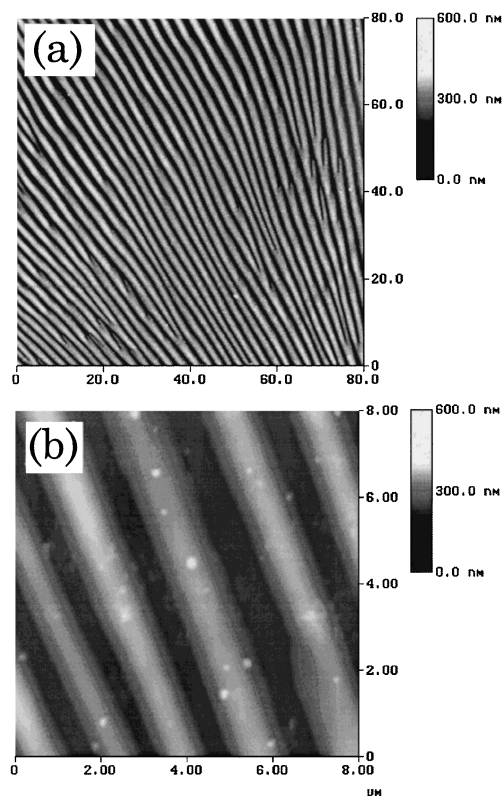


Fig. 2. (a) Copper wires grown on silicon wafer viewed by atomic force microscopy. During the electrodeposition the voltage across the electrodes was maintain at 5.0 V and the temperature was  $-4^\circ\text{C}$ . (b) Copper wires viewed with a higher magnification.

ments also showed that the average width of the copper wires depended on the voltage applied across the electrodes (actually the strength of the local electric field). The higher applied voltage usually made the copper wires broader.

A transmission electron microscope (TEM; JEM-4000EX, JOEL, Japan) was used to characterize both the microstructure and the composition of the copper wires. Figure 3(a) illustrates the diffraction contrast image of the copper wire, where the crystallites are less than 40 nm in size. The diffraction pattern of the copper wire is demonstrated in Fig. 3(b), which indicates that the nanocrystallites in the wire are randomly orientated. It is noteworthy that in addition to the diffraction of copper, the diffraction of  $\text{Cu}_2\text{O}$  can be identified. According to the literature,<sup>22-25</sup> the generation of  $\text{Cu}_2\text{O}$  depends on the pH of the solution, as well as on the electrode potential. In our case the pH of the electrolyte was 4.5 and the applied voltage was 10 volts, but  $\text{Cu}_2\text{O}$  still existed. However, the shiny metallic color of the copper deposit suggested that the percentage of  $\text{Cu}_2\text{O}$  in the copper wire was not high. This argument was supported by the resistivity measurements. To measure the electric resistivity of the copper wires, a bunch of seven long, parallel copper wires grown on an ordinary glass substrate (cover glass) was selected while the neighboring wires were carefully removed under an optical microscope. A line mask 80  $\mu\text{m}$  in width was placed perpendicularly across the copper wires and the conducting copper film

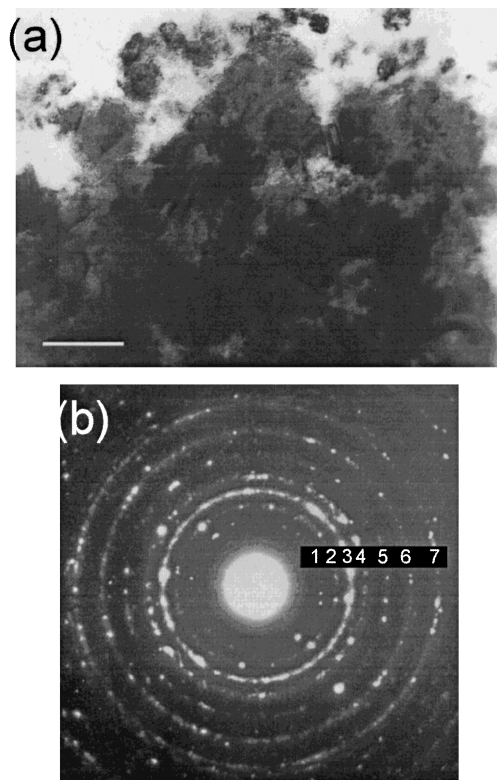


Fig. 3. (a) Electron diffraction contrast micrograph of the copper wire. The crystallite in the wire is of the order of 20 nanometers. The bar represents 50 nm. (b) The electron diffraction pattern of the copper wire, where the diffraction of both copper and  $\text{Cu}_2\text{O}$  can be identified. Numbers on the diffraction rings represent: (1)  $\text{Cu}_2\text{O}$  (110); (2)  $\text{Cu}_2\text{O}$  (111); (3) Cu (111); (4) Cu (200); (5)  $\text{Cu}_2\text{O}$  (220); (6) Cu (220); (7) Cu (311).

was deposited on the sample by magnetron sputtering. Thereafter the line mask was removed, thus a sample of seven copper wires in parallel, connected by two conducting copper films, was ready for the measurement (by the two-probe method). It was found that at room temperature the electric resistance was  $10.35 \Omega$ . The exact length and the cross-section area of the copper wires between the two conducting films were determined by AFM measurements. It followed that the room-temperature resistivity of the copper wires was  $52 \mu\Omega \cdot \text{cm}$ . This value was nearly 30 times higher than that of pure copper.<sup>26)</sup> One possible explanation for the higher resistivity is the presence of  $\text{Cu}_2\text{O}$  in the copper wires, as indicated in Fig. 3(b). Switzer *et al.*<sup>27)</sup> studied the resistivity as a function of the percentage of copper in a multilayer sample of Cu/ $\text{Cu}_2\text{O}$ . According to their data, when the sample contains 2%  $\text{Cu}_2\text{O}$ , the resistivity is  $81 \mu\Omega \cdot \text{cm}$ . It can be inferred that the concentration of  $\text{Cu}_2\text{O}$  in our sample is much lower than 2%. The higher resistivity of our sample may also be due to use of the two-probe measuring method, in which the contact resistance, although every small, was not eliminated. Efforts are being devoted now to establish a four-probe contact to a copper wire by means of photolithography.

We were interested in the thermal stability of the copper wires. To study the dynamic behavior of the electric resistance of the copper wires under annealing,

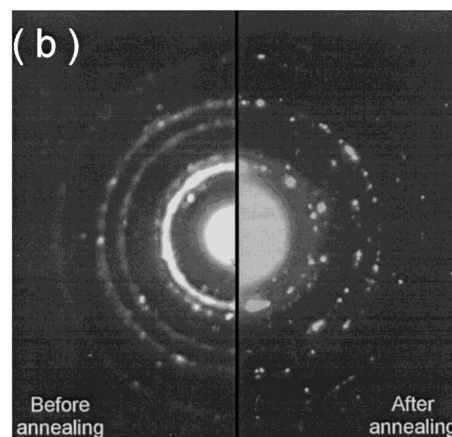
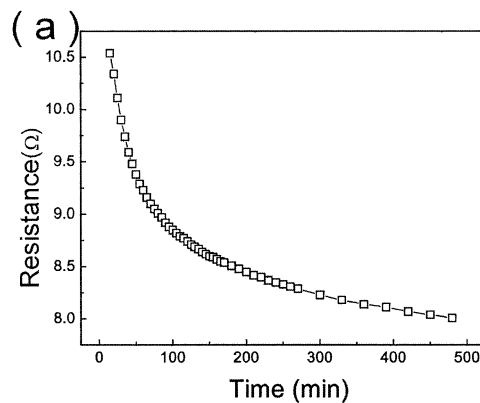


Fig. 4. (a) Electric resistance of seven copper wires in parallel measured at  $200^\circ\text{C}$  as a function of time. For this measurement the copper wires were grown on the surface of a cover glass. In the first 100 min the resistance decreases with a higher rate, then it drops with a lower rate. (b) The electron diffraction pattern of a copper wire before and after annealing at  $200^\circ\text{C}$ . The field diagram was kept the same for these two scenarios. After annealing the separated diffraction dots become more evident.

the sample was kept at  $200^\circ\text{C}$  for 8 h in a vacuum of  $2.0 \times 10^{-6}$  Torr. The resistance of the sample was measured *in situ* during the annealing process. As shown in Fig. 4(a), the resistance decreased quickly in the first 100 min, and thereafter it dropped at a lower rate. We expected that the density of grain boundaries in the copper wires was decreased by annealing. Thus the resistance of the copper wires was lowered by about 24% by annealing for 8 h. Figure 4(b) provides support for this argument, where the electron diffraction patterns of the same sample before and after annealing are presented. It is clear that before annealing, the orientation of the crystallite in the copper was almost random, so rings existed in the diffraction pattern; after annealing, however, this feature was weakened. Instead of the rings, many separated, bright dots dominated the diffraction pattern, suggesting that the number of the crystallites had been significantly decreased. It should be noted from Fig. 4(a) that the reduction of the resistance was still not saturated after 8 h of annealing. This implies that the reconstruction of the microstructures in the copper wires was continuous throughout.

Since the early study of the ramified pattern in electrodeposition by Matsushita *et al.*,<sup>28)</sup> much progress has

been made in understanding the formation of various patterns in electrodeposition.<sup>15)</sup> Recently we noted the reports on the localized electrochemical deposition of copper columns and interconnects from the acid sulfate solutions,<sup>29,30)</sup> where the width of the copper deposit was larger than ours. Our experiment differs from previous ones in the introduction of an ultrathin electrodeposition system, in which the convective disturbance and the diffusive instability in front of the growing tips are suppressed significantly.<sup>31)</sup> As a result, the tip-splitting rate is decreased, and the deposit morphology changes from fractal-like or dense-branching morphology to the smooth, less-branched array of copper filaments. The formation of the array of copper filaments is a spontaneous process without using additives or templates. When the density of the growing tip is high, i.e., if the separation of the filaments is significantly smaller than the thickness of the concentration boundary layer, the concentration field in front of each individual tip is significantly overlapped. In this case, the growing tips actually encounter a one-dimensional concentration field. The competition for the nutrient supply among the growing tips may cause screening of some tips. The screened tips are trapped and stop growing. If, however, the separation of the copper wires is much larger than the concentration boundary layer, the concentration field in front of each individual tip is two-dimensional. In this case, the width of the copper wire will increase gradually. At a certain threshold, tip-splitting may occur. In this way, the separation of the copper filaments is spontaneously adjusted. This depends on the thickness of the electrolyte solution and the electric field. As a matter of fact, the recent experimental observations by Argoul *et al.*<sup>32)</sup> have illustrated that periodicity among the neighboring deposit branches does exist. However, for the conventional electrodeposition in aqueous electrolyte film, the electrodeposits are ramified, hence it is difficult to identify this periodicity unless some mathematical transformation is applied.<sup>32)</sup> By suppressing the ramification of the electrodeposit branches, the array of nearly straight copper wires is demonstrated for the first time in this report.

To conclude, we report here the formation of straight copper wire arrays by electrochemical deposition on silicon substrate. We suggest that the extremely low branching rate of the copper deposit is due to the suppression of disturbances at the growth front in our ultrathin electrochemical deposition system. The phenomenon reported here is enlightening for the understanding of pattern formation under far-from-equilibrium conditions. In addition, it also promises a simple and cost-effective way to fabricate straight, narrow copper wires on silicon substrate without using additives or templates, and without resorting to photolithography. Furthermore, we expect that this wire-fabrication method is not limited to copper only, it is expected to be applicable to the electrodeposition of other metals as

well.

This work was supported by the Ministry of Science and Technology of China via the State Key Program for Basic Researches, and by the Natural Science Foundation of China. The support of the Qiu Shi Foundation of Science and Technology (Hong Kong) is also acknowledged. The author is grateful to the Physical Society of Japan for financial support in publication.

- 1) D. Edelstein *et al.*: Tech. Dig. Int. Electron. Devices Meet., IEEE, Washington D.C., 1997, p. 773.
- 2) S. Venkatesan *et al.*: Tech. Dig. Int. Electron. Devices Meet., IEEE, Washington D.C., 1997, p.769.
- 3) D. Edelstein: Proc. VMIC **12** (1995) 301.
- 4) V. Fleury and D. Barkey: Europhys. Lett. **36** (1996) 253.
- 5) V. Fleury and D. Barkey: Physica A **233** (1996) 730.
- 6) J. J. Kelly, C. Tian and A. C. West: J. Electrochem. Soc. **146** (1999) 2540.
- 7) R. Winand: Electrochim. Acta **39** (1994) 1091.
- 8) G. A. Hope, G. M. Brown, D. P. Schweinsberg, K. Shimizu and K. Kobayashi: J. Appl. Electrochem. **25** (1995) 890.
- 9) C. Gurtner and M. J. Sailor: Adv. Mater., **8** (1996) 897.
- 10) J.-C. Bradley, H.-M. Chen, J. Crawford, J. Eckert, K. Er-nazarova, T. Kurzeja, M. Lin, M. McGee, W. Nadler and S. G. Stephens: Nature **389** (1997) 268.
- 11) C. L. Curtis, J. E. Ritchie and M. J. Sailor: Science **262** (1993) 2014.
- 12) M. J. Sailor and C. L. Curtis: Adv. Mater. **6** (1994) 688.
- 13) V. Fleury: Nature **390** (1997) 145.
- 14) J. Nittmann and H. E. Stanley: Nature **321** (1986) 663.
- 15) E. Ben-Jacob and P. Garik: Nature **343** (1990) 523.
- 16) E. Ben-Jacob: Contemp. Phys. **34** (1993) 247.
- 17) S.-C. Huang and M. E. Glicksman: Acta Metall. **29** (1981) 717.
- 18) R. Pieters and J. S. Langer: Phys. Rev. Lett. **56** (1986) 1948.
- 19) X. W. Qian and H. Z. Cummins: Phys. Rev. Lett. **64** (1990) 3038.
- 20) A. A. Chernov: *Modern Crystallography III: Crystal Growth* (Springer-Verlag, Berlin, 1984)
- 21) N.-B. Ming: *Fundamentals of Crystal Growth Physics* (Shanghai Science and Technology, Shanghai, 1982) p. 45.
- 22) J. A. Switzer, C.-J. Hung, L.-Y. Huang, E. R. Switzer, D. R. Kammler, T. D. Golden and E. W. Bohannon: J. Am. Chem. Soc. **120** (1998) 3530.
- 23) F. Texier, L. Servant, J. L. Bruneel and F. Argoul: J. Electroanal. Chem. **446** (1998) 189.
- 24) M. Lopez-Salvans, F. Sagues, J. Claret and J. Bassas: J. Electroanal. Chem. **421** (1997) 205.
- 25) Da-ling Lu and Hen-ichi Tanaka: J. Electrochem. Soc. **143** (1996) 2105.
- 26) *CRC Handbook of Chemistry and Physics* (CRC Press, Boca Raton, 1995) 76th ed., p. 12.
- 27) J. A. Switzer, C.-J. Hung, L.-Y. Huang, F. S. Miller, Y. Zhou, E. R. Raub, M. G. Shumsky and E. W. Bohannon: J. Mater. Res. **13** (1998) 909.
- 28) M. Matsushita, M. Sano, Y. Hayakawa, H. Honjo and Y. Sawada: Phys. Rev. Lett. **53** (1984) 286.
- 29) E. M. El-Giar, R. A. Said, G. E. Bridges and D. J. Thomson: J. Electrochem. Soc. **147** (2000) 586.
- 30) J.-C. Bradley, J. Crawford, M. McGee and S. G. Stephens: J. Electrochem. Soc. **145** (1998) L45.
- 31) M. Wang, S. Zhong, X.-B. Yin, J.-M. Zhu, R.-W. Peng, Y. Wang, K.-Q. Zhang and N.-B. Ming: Phys. Rev. Lett. **86** (2001) 3827.
- 32) C. Leger, J. Elezgaray and F. Argoul: Phys. Rev. E **61** (2000) 5452.